



A formal scan rate in staircase and square-wave voltammetry

Dijana Jadreško, Marina Zelić*, Milivoj Lovrić

Department for Marine and Environmental Research, Ruđer Bošković Institute, PO Box 180, 10002 Zagreb, Croatia

ARTICLE INFO

Article history:

Received 18 January 2010

Received in revised form 29 March 2010

Accepted 19 April 2010

Available online 24 April 2010

Keywords:

Formal scan rate

Staircase voltammetry

Square-wave voltammetry

Potential step increment

ABSTRACT

Because of the fact that real measurements are sometimes described in terms of the (formal) scan rate, the functional relationships between this parameter and the peak current in staircase (SCV) and square-wave voltammetry (SWV) were investigated theoretically. The real SCV peak current is proportional to the square-root of the formal scan rate, v , and inversely proportional to $\Delta E^{0.0541}$: $-i_p = 0.1453nFSc_{ox}^*(D/\pi)^{1/2}v^{1/2}\Delta E^{-0.0541}$. In SWV of a reversible electrode reaction the net peak current depends primarily on the frequency, while the influence of the formal scan rate is of minor importance: $\Delta i_p = nFSc_{ox}^*D^{1/2}(0.7339f^{1/2} + 0.0026\Delta E^{0.3118}v^{1/2})$. On the other hand, in SWV of a totally irreversible electrode reaction, the real net peak current is a stronger function of the formal scan rate: $\Delta i_p = 0.0942nFSc_{ox}^*D^{1/2}\Delta E^{-0.11}v^{1/2}$. Experimental results, obtained in perchlorate solutions of Eu^{3+} , are in relatively good agreement with the theory.

© 2010 Elsevier B.V. All rights reserved.

1. Introduction

The main characteristic of modern voltammetric techniques is a stepwise change of the electrode potential [1]. A staircase potential – time waveform is a basic signal to which potential pulses are superimposed in pulse, differential pulse (DPV) [2] and square-wave voltammetry (SWV) [3]. The staircase excitation signal is defined by the potential step increment, ΔE , and the step duration, τ . These two independent variables define a formal scan rate, $v = \Delta E/\tau$. The staircase current response depends also on sampling parameter, γ , which is the fraction of step at which the current is measured ($0 < \gamma < 1$) [4,5]. It is well known that the variation of the scan rate with following of the resulting signals is an important method in investigation of mechanisms of electrode processes, especially in the linear scan voltammetry, LSV [6,7]. More precisely, (apparent) reversibility depends on the time scale of experiment, i.e. on the scan rate in LSV or cyclic voltammetry. Therefore, appearance of a redox process can be changed from reversible to quasireversible by increasing the scan rate. However, it is generally accepted that, unlike the scan rate dE/dt in LSV, the formal scan rate is not a meaningful parameter in staircase voltammetric (SCV) [4] and square-wave voltammetric experiments [8] because there are many combinations of ΔE and τ , (or frequency, f) which can give the same particular value of v while at the same time differing in the current response. Furthermore, the characteristic time of SWV experiment depends only on frequency and not on $v = f\Delta E$ [9]. Nevertheless, some authors quote the scan rate as a relevant

parameter in description of SWV [10,11] or even DPV experiments [12].

In a number of studies the effects of variation of ΔE , τ , and γ on the SCV current response were investigated in order to find the conditions under which it is the same as in LSV for a wide variety of mechanisms [4,5,13–17]. Also, there are many papers in which the effect of kinetic (α) and experimental parameters (e.g. ΔE , E_{sw} , f) on the square-wave voltammograms have been investigated [3,8,9,18,19]. However, little is known about the influence of formal scan rate on peak currents in SCV and SWV. In this communication, the functional relationships between the peak current and formal scan rate (in both techniques) are investigated by numerical simulation of simple, reversible and totally irreversible electrode reactions. The value of potential step increment was changed from 0.1 to 10 mV, and from 0.1 to 30 mV in the case of SCV and SWV, respectively. Some results were compared with experimentally obtained relationships.

2. Experimental

All solutions were prepared from the reagent grade chemicals and water purified in a Millipore Milli-Q system.

Square-wave voltammograms were recorded using a static mercury drop electrode PAR 303 (Princeton Applied Research) attached to a μ Autolab System (Eco Chemie, Utrecht). Platinum wire served as a counter electrode whereas all potentials were given with respect to the saturated Ag/AgCl(NaCl) reference electrode.

Before recording each new set of voltammograms, the solution in the polarographic cell was deaerated with high purity (99.999%) nitrogen for 15 min. The room temperature was kept at 25 °C.

* Corresponding author. Tel.: +385 14561181; fax: +385 14680242.

E-mail address: zelic@irb.hr (M. Zelić).

3. The model

A simple, reversible reaction on the stationary, planar electrode was considered:



It was assumed that both the reactant Ox and product Red were soluble in aqueous electrolyte solution. For semi-infinite linear diffusion the following system of differential equations and boundary conditions has to be solved:

$$\frac{\partial c_{\text{Ox}}}{\partial t} = D \frac{\partial^2 c_{\text{Ox}}}{\partial x^2}; \quad \frac{\partial c_{\text{Red}}}{\partial t} = D \frac{\partial^2 c_{\text{Red}}}{\partial x^2} \quad (2)$$

$$t = 0, \quad x \geq 0: \quad c_{\text{Ox}} = c_{\text{Ox}}^*, \quad c_{\text{Red}} = 0 \quad (3)$$

$$t > 0, \quad x \rightarrow \infty: \quad c_{\text{Ox}} \rightarrow c_{\text{Ox}}^*, \quad c_{\text{Red}} \rightarrow 0 \quad (4)$$

$$x = 0: \quad D \left(\frac{\partial c_{\text{Ox}}}{\partial x} \right)_{x=0} = -D \left(\frac{\partial c_{\text{Red}}}{\partial x} \right)_{x=0} \equiv -\frac{i}{nFS} \quad (5)$$

$$(c_{\text{Ox}})_{x=0} = \exp(\varphi) \cdot (c_{\text{Red}})_{x=0} \quad (6)$$

The application of the Feldberg's *finite difference* approximation [20] to Eq. (5) gives the expression:

$$\frac{cox(1) - cox(0)}{\frac{\Delta x}{2}} = -\frac{cred(1) - cred(0)}{\frac{\Delta x}{2}} \equiv -\frac{i}{nFS c_{\text{Ox}}^* D} \quad (7)$$

where symbols $cox(0)$ and $cred(0)$ denote the concentrations of Ox and Red species immediately at the electrode surface, respectively, while the symbols $cox(1)$ and $cred(1)$ correspond to concentrations of Ox and Red species in the middle of the first space increment.

Introducing Eq. (7) into Eq. (6) yields the expression for the “operating” dimensionless current:

$$\frac{i\Delta t}{nFS c_{\text{Ox}}^* \Delta x} = -2 \frac{dd}{1 + e^\varphi} [cox(1) - e^\varphi cred(1)] \quad (8)$$

where $dd \equiv D\Delta t/\Delta x^2 = 0.4$ is a dimensionless diffusion coefficient, Δx and Δt are the space and time increments, respectively, $\varphi = nF(E - E^0)/RT$ is dimensionless potential and n is the number of electrons. The meanings of all symbols are given in the Table 1.

The dimensionless SCV current was calculated by using $\Delta t = \tau/250$ and multiplying Eq. (8) with $5\sqrt{10\pi}/\sqrt{dd}$, where $\tau = \Delta E/\nu$ is a stair-case period:

$$\Phi = i\sqrt{\pi\tau}/(nFS c_{\text{Ox}}^* \sqrt{D}) \quad (9)$$

The similar expression for the dimensionless SWV current was obtained by using $\Delta t = \tau/25$ where $\tau = 1/2f$ (i.e. each square-wave half-period is divided into 25 time increments) and multiplying Eq. (8) with $5\sqrt{2}/\sqrt{dd}$:

$$\Phi = i/(nFS c_{\text{Ox}}^* \sqrt{Df}) \quad (10)$$

In case of totally irreversible electrode reaction (i.e. slow charge transfer: $\text{Ox} + n\text{e}^- \rightarrow \text{Red}$), the mathematical formulation includes Eqs. (2)–(5), but the Eq. (6) must be substituted by:

$$i/nFS = -k_s \exp(-\alpha\varphi) (c_{\text{Ox}})_{x=0} \quad (11)$$

where k_s is the standard rate constant and α is the cathodic transfer coefficient. In this case, the following SW dimensionless “operating” current is obtained:

$$\frac{i\Delta t}{nFS c_{\text{Ox}}^* \Delta x} = -\frac{\kappa \cdot e^{-\alpha\varphi} \cdot cox(1)}{1 + \frac{\kappa \cdot e^{-\alpha\varphi}}{2dd}} \quad (12)$$

where $\kappa = \lambda \cdot \sqrt{dd}/5\sqrt{2}$ and $\lambda = k_s/\sqrt{Df}$ is a dimensionless kinetic parameter. Again, multiplying this expression (Eq. (12)) with $5\sqrt{2}/\sqrt{dd}$, the dimensionless SWV current is obtained (Eq. (10)).

Table 1
List of symbols.

c_{Ox}	Concentration of the reactant
c_{Ox}^*	Bulk concentration of the reactant
$(c_{\text{Ox}})_{x=0}$	Concentration of the reactant at the electrode surface
c_{Red}	Concentration of the product
dd	Dimensionless diffusion coefficient
D	Diffusion coefficient
E	Electrode potential
E_{st}	Starting potential
E^0	Standard electrode potential
E_{SWV}	SW amplitude
f	SW frequency
i	Current
n	Number of electrons
F	Faraday constant
R	Gas constant
S	Electrode surface area
k_s	Standard rate constant
t	Time
t_{int}	Integration period
Δt	Time increments
T	Absolute temperature
ν	Scan rate
x	Space coordinate
Δx	Space increments
ΔE	Potential step increment
Φ	Dimensionless current
Φ_p	Dimensionless SCV peak current
$\Delta\Phi_p$	Dimensionless SWV net peak current
α	Cathodic charge transfer coefficient
$\lambda = k_s (Df)^{-1/2}$	Dimensionless kinetic parameter
τ	Step duration
$\gamma = [1 + (1 - t_{\text{int}}/\tau)]/2$	Sampling parameter

4. Results and discussions

4.1. Staircase voltammetry (SCV)

The theoretical treatment of SCV for the reversible system was presented by Christie and Lingane [13], more than 40 years ago. In the meantime SCV and LSV were compared (theoretically and experimentally) in many papers. They presented a combination of experimental (e.g. ΔE) and sampling (γ) parameters which gave equal voltammograms in SC and LS voltammetry [4,14–17,21]. On the other hand, little is known about the effect of scan rate on the SC peak current. According to Christie and Lingane, the peak current depends linearly on $\tau^{-1/2}$ and approximately linearly on $\Delta E^{1/2}$ [13].

In this paper, the influence of the formal scan rate on dimensionless peak current, Φ_p , was tested theoretically by changing the potential step increment, ΔE , for reversible electrode reaction (1). In the first type of calculations, the current was measured at the end of each step ($\gamma = 1$). The effect of ΔE on the dimensionless SCV peak current is presented in Fig. 1A and 1B. It is shown that the absolute value of dimensionless peak current increases with increasing potential step increment (Fig. 1A). The circles are results of numerical simulation and the interconnecting line is the best fit: $-\Phi_p = 0.1453 \Delta E^{0.4459}$. The precision of fitting procedure can be seen in Fig. 1B, in which a linear relationship between dimensionless peak current and $\Delta E^{0.4459}$ is shown. In a recently published paper [22] the same dependence was described by an equation: $-\Phi_p = 0.4463/(1 + 0.375X^{0.52})$, where $X = nF\Delta E/RT$. At first glance it does not seem to be in agreement with our results. The point is that Φ , in comparison with Eq. (9), was defined in a somewhat different way. The values from Fig. 1A, however, could be perfectly fitted ($R = 1.0000$) by a function of this type ($-\Phi_p = A/(B + C\Delta E^D)$), although the constants (and their physical meanings) differ significantly from those in the literature example. The resulting curve, with $D = -0.503$ is given in Fig. 1A by a red line.

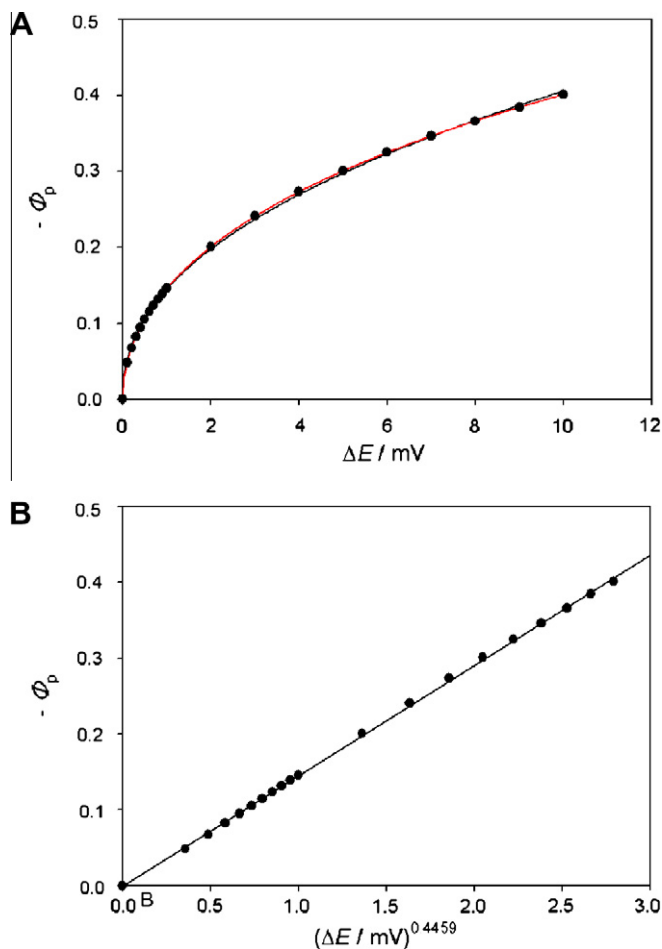


Fig. 1. Dependence of the dimensionless staircase voltammetric (SCV) peak current on potential step increment, ΔE , (A) and on $\Delta E^{0.4459}$ (B). The best fit of calculated data (●) to theoretical function $-\Phi_p = 0.1453 \Delta E^{0.4459}$ is given (black line) together with the best fit to the function $-\Phi_p = A/(B + C\Delta E^D)$ (red line). The current sampling fraction $\gamma = 1$, the initial potential $E_{st} = 0.3$ V vs. E^0 and $n = 1$. (For interpretation of the references to colour in this figure legend, the reader is referred to the web version of this article.)

By introducing Eq. (9) into the current function: $-\Phi_p = 0.1453 \Delta E^{0.4459}$, we observe that the real SCV peak current is proportional to the square-root of the formal scan rate and inversely proportional to $\Delta E^{0.0541}$:

$$-i_p = 0.1453nFSc_{ox}^* \sqrt{D/\pi} \sqrt{\nu} \Delta E^{-0.0541} \quad (13)$$

where $\nu = \Delta E/\tau$. Eq. (13) applies for the constant ΔE and variable step duration. If ΔE is varied and τ is constant, the peak current can be expressed as a function of these two variables:

$$-i_p \propto \Delta E^{0.4459} \tau^{-0.5} \quad (14)$$

In SCV experiments the current is integrated during a certain interval at the end of each potential step and the average current is reported:

$$\bar{i} = \frac{1}{t_{int}} \int_{\tau-t_{int}}^{\tau} i dt \quad (15)$$

where t_{int} is the integration period. Considering Eq. (9), the average current is defined by the following equation:

$$\bar{i} = 2k\Phi(\sqrt{\tau} - \sqrt{\tau - t_{int}})t_{int}^{-1} \quad (16)$$

where $k = nFSc_{ox}^* \sqrt{D/\pi}$ and Φ is a certain function of electrode potential. By multiplying both numerator and denominator in Eq. (16) by $(\sqrt{\tau} + \sqrt{\tau - t_{int}})$ one obtains:

$$\bar{i} = \frac{k\Phi}{\gamma\sqrt{\tau}} \quad (17)$$

$$\gamma = \frac{1 + \sqrt{1 - \frac{t_{int}}{\tau}}}{2} \quad (18)$$

The sampling parameter γ decreases from $\gamma = 1$, for $t_{int} = 0$, to $\gamma = 0.5$ for $t_{int} = \tau$. This procedure was simulated by the summation of dimensionless currents during the last m time increments of each pulse and by calculating the average dimensionless current:

$$\bar{\Phi} = \frac{1}{m} \sum_{250-m}^{250} \Phi \quad (19)$$

The period of integration was changed from $t_{int}/\tau = 0.02$ to $t_{int}/\tau = 0.4$, which corresponded to the variation of γ from 0.995 to 0.887, respectively. Fig. 2 shows linear relationship between the average dimensionless SCV peak current and the reciprocal of the sampling parameter:

$$-\bar{\Phi} = 0.2681 + 0.1332 \frac{1}{\gamma} \quad (20)$$

If $\gamma = 1$, the average peak current is equal to 0.4013, which is the value of instantaneous peak current corresponding to $\Delta E = 10$ mV (see the last point in Fig. 1A).

The current-sampling procedure has no significant influence on the relationship between the real SCV peak currents and the potential step increment. Fig. 3 shows the dependence of the average dimensionless SCV peak currents on the potential step increment for three integration periods. These relationships can be described by the following functions: $-\bar{\Phi}_p = 0.1453\Delta E^{0.4467}$ for $t_{int}/\tau = 0.04$, $-\bar{\Phi}_p = 0.1461\Delta E^{0.4507}$ for $t_{int}/\tau = 0.2$, and $-\bar{\Phi}_p = 0.1473\Delta E^{0.4565}$ for $t_{int}/\tau = 0.4$. For the last integration period the real peak current depends on the square-root of the formal scan rate and on $\Delta E^{-0.0435}$. So, the longer integration period is, the smaller is the difference between the staircase voltammetry and linear scan voltammetry.

4.2. Square-wave voltammetry (SWV)

The influence of the formal scan rate ($\nu = f \Delta E$) on the dimensionless net peak current, $\Delta\Phi_p$, was tested by changing the step increment, ΔE , for reversible and totally irreversible electrode processes. The dimensionless current was calculated at the end of each SW half-period using Eqs. (8) and (10), and $\Delta\Phi > 0$ was arbitrary

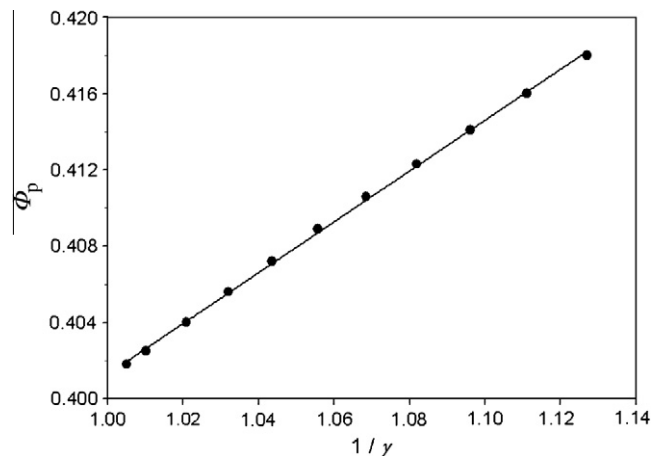


Fig. 2. Dependence of the average dimensionless SCV peak current on the reciprocal of the sampling parameter. The results of simulation are points and the line is a linear relationship $-\bar{\Phi}_p = 0.2681 + 0.1332\gamma^{-1}$. $E_{st} = 0.3$ V vs. E^0 , $\Delta E = 10$ mV, $n = 1$.

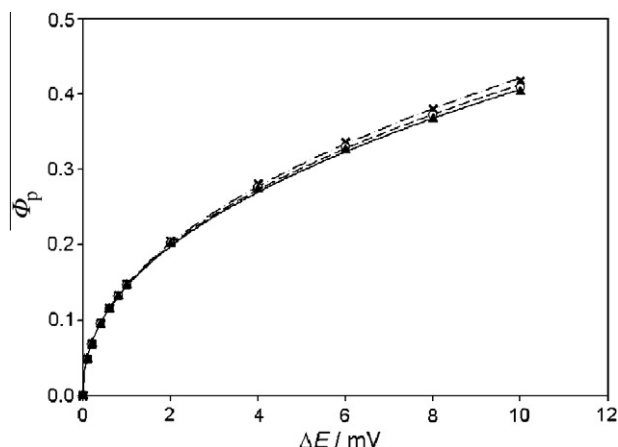


Fig. 3. Dependence of the average dimensionless SCV peak current on the potential step increment for three times of integration: $t_{int}/\tau = 0.04$ (▲), 0.2 (○) and 0.4 (x). The lines are the best fittings by the function $y = ax^b$. All parameters are as in Fig. 2.

chosen for reduction reaction. (The consequences of current sampling at different pulse fractions were described previously [23,3].) The difference in potential of the forward and backward pulses is $2E_{sw} = 100$ mV.

Dependence of the dimensionless net peak current on the potential step increment is shown in Fig. 4A and 4B for reversible electrode reaction (1). The solid line in each instance is the best fitting curve. It is shown that for $\Delta E \geq 0.1$ mV this relationship is a power function:

$$\Delta\Phi_p = 0.7339 + 0.0026\Delta E^{0.8118} \quad (21)$$

Fig. 4B shows that the linear relationship between $\Delta\Phi_p$ and $\Delta E^{0.8118}$ exists in the wide range $0.1 \leq \Delta E/\text{mV} \leq 30$. The intercept 0.7339 is an extrapolation of the function (21) to $\Delta E = 0$ mV and has no physical meaning because $\Delta\Phi_p = 0$ for $\Delta E = 0$ mV (see the first point in Fig. 4A). However, for all practical purposes ($\Delta E > 0.1$ mV) the dimensionless net peak current is defined by Eq. (21). This offset is a reason that the influence of ΔE on the $\Delta\Phi_p$ is not significant. It was found that the value of $\Delta\Phi_p$ increased by only 5% (from 0.7345 to 0.7741) with the increasing of ΔE from 0.1 mV to 30 mV. The intercepts of these curves depend on the value of SW amplitude, E_{sw} , as can be seen in Fig. 5. The relationships in this figure are the following: $\Delta\Phi_p = 0.4407 + 0.0052\Delta E^{0.7274}$ for $E_{sw} = 25$ mV, $\Delta\Phi_p = 0.6374 + 0.0035\Delta E^{0.7709}$ for $E_{sw} = 40$ mV, and $\Delta\Phi_p = 0.8787 + 0.0011\Delta E^{0.9326}$ for $E_{sw} = 75$ mV.

Introducing Eq. (10) into the current function (21) gives the real net peak current as a function of frequency, the formal scan rate and the potential step increment:

$$\Delta i_p = nFSc_{ox}^* \sqrt{D} (0.7339 \sqrt{f} + 0.0026 \Delta E^{0.3118} \sqrt{v}) \quad (22)$$

where $v = f\Delta E$. The reason for this relationship is the regeneration of the reactant by the reoxidation of the product during the backward, anodic pulse. So, in the vicinity of the working electrode surface the reactant is not exhausted by the slow scan rate as it is in staircase voltammetry. This explanation is confirmed by the lack of the offset in SWV of totally irreversible electrode reactions, in which there is no reoxidation of the product.

The effect of ΔE on the dimensionless SWV net peak current, for irreversible electrode reaction, is presented in Fig. 6A and 6B. The dimensionless current was calculated using Eqs. (12) and (10) for $\lambda = 0.001$ and $\alpha = 0.5$. This value of dimensionless kinetic parameter λ corresponds to totally irreversible reaction (i.e. to the standard rate constant $k_s = 10^{-5}$ cm s⁻¹ if $D = 10^{-6}$ cm² s⁻¹ and a typical value of SW frequency $f = 100$ Hz is used). As can be seen, unlike in

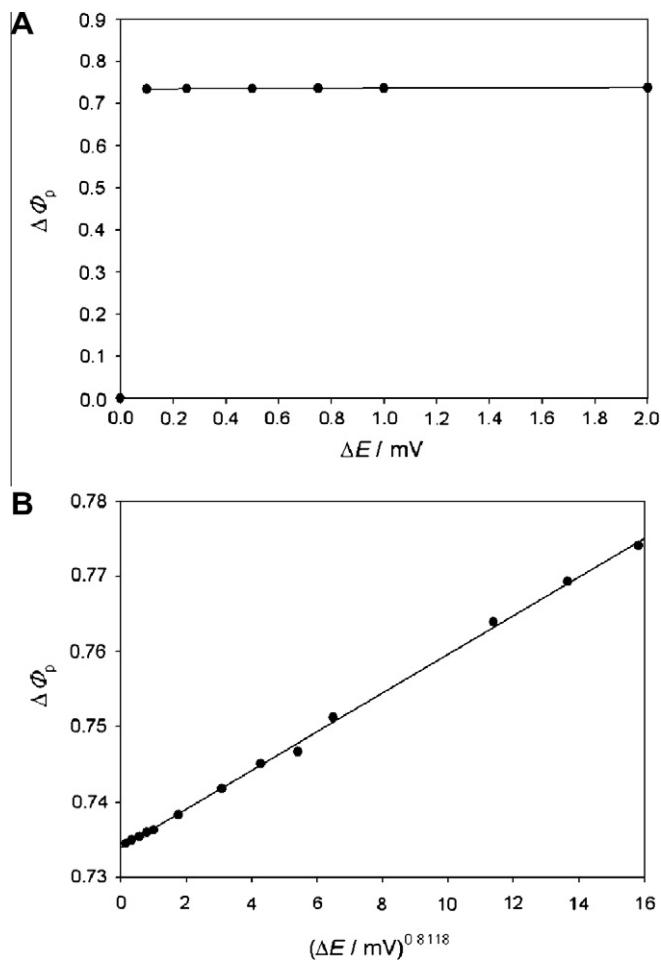


Fig. 4. Dependence of the dimensionless SWV net peak current on the potential step increment for the reversible electrode reaction. (A) The best fit of the results of simulation (●) to the theoretical function $\Delta\Phi_p = 0.7339 + 0.0026 \Delta E^{0.8118}$, for $\Delta E \geq 0.1$ mV (—). (B) Linear relationship between dimensionless net peak current and $\Delta E^{0.8118}$. The current sampling fraction is $\gamma = 1$, $E_{st} = 0.3$ V vs. E^0 , $n = 1$ and $E_{sw} = 50$ mV.

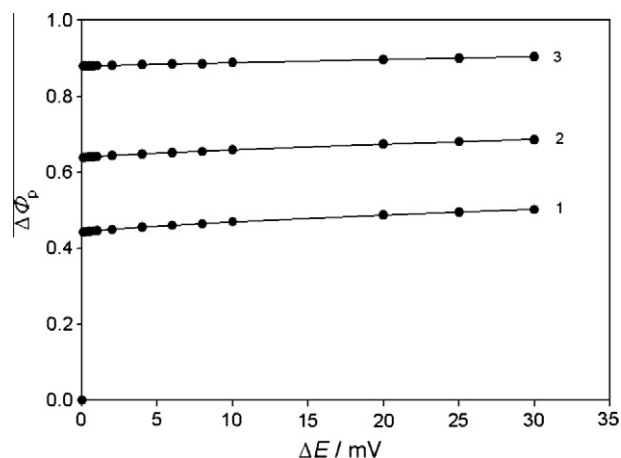


Fig. 5. Dependence of the dimensionless SWV net peak current on the potential step increment for three values of SW amplitude: $E_{sw}/\text{mV} = 25$ (1), 40 (2) and 75 (3). All other parameters are as in Fig. 4.

the reversible processes, the influence of potential step increment on the net peak current is pronounced and $\Delta\Phi_p$ increases consid-

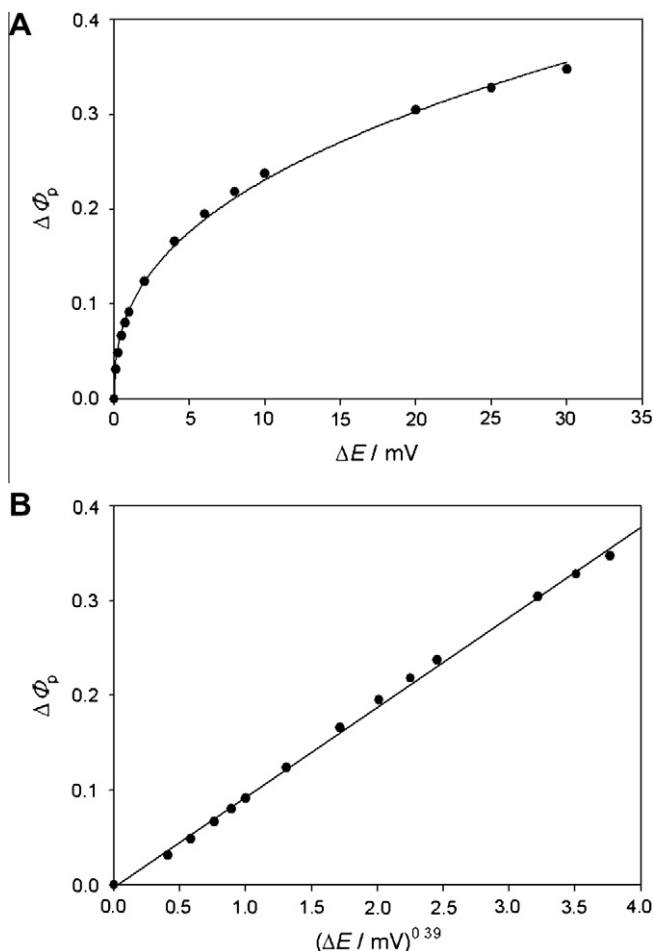


Fig. 6. Dependence of the dimensionless SWV net peak current on the potential step increment for irreversible reaction. (A) The best fit of the results of simulation (●) to the theoretical function $\Delta\Phi_p = 0.0942 \Delta E^{0.39}$ (—). (B) Linear relationship between dimensionless net peak current and $\Delta E^{0.39}$. The current sampling fraction is $\gamma = 1$, $E_{st} = 0.3$ V vs. E^0 , $n = 1$, $E_{sw} = 50$ mV, $\alpha = 0.5$ and $\lambda = 0.001$.

erably with the small increase of ΔE . This dependence can be described by the following function:

$$\Delta\Phi_p = 0.0942\Delta E^{0.39} \quad (23)$$

This relationship was confirmed by real measurements, in which reduction of Eu^{3+} to Eu^{2+} [24,25] was taken as a model (Fig. 7).

The real net peak current can be interpreted as a function of the formal scan rate:

$$\Delta i_p = 0.0942nFSc_{ox}^* \sqrt{D}\Delta E^{-0.11} \sqrt{\nu} \quad (24)$$

This expression is similar to the Eq. (5) given by Fatouros and Krulic [26]. Although their result was originally written in a somewhat different form, it implies the dependence of the real peak current on $\nu^{1/2}\Delta E^{-0.09}$ which is similar to our conclusion.

The expression (24) is more alike to SCV than to SWV of reversible reaction, which indicates that the influence of formal scan rate on the responses of these techniques originates from the development of deep diffusion layer at the working electrode surface. Experimental results, obtained with Eu^{3+} in acidified 1 mol/l NaClO_4 , are in qualitative agreement with Eq. (24) (Fig. 8). The peak current (measured at a constant value of the step potential and gradually increasing SW frequency) is a linear function of $\nu^{1/2}$ but the resulting straight line does not pass through the origin. The intercept is without physical meaning, whereas its origin stays

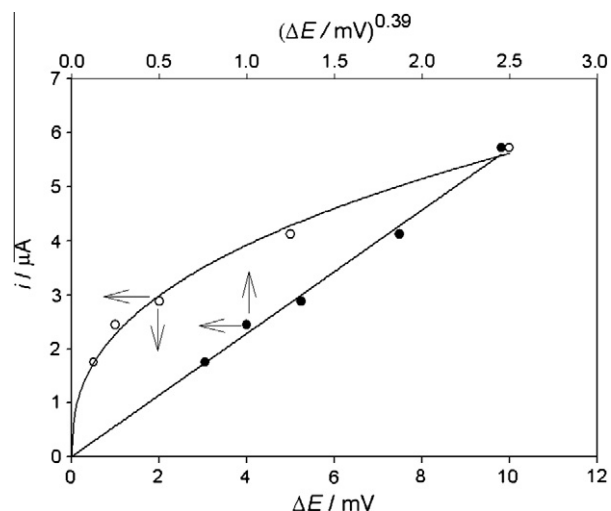


Fig. 7. Dependence of the real SW peak current on the potential step increment (ΔE) and on $\Delta E^{0.39}$. Solution composition: 0.5 mmol/l Eu^{3+} , 0.1 mol/l NaClO_4 , 0.01 mol/l HClO_4 . SW amplitude: 40 mV; SW frequency: 100 s^{-1} .

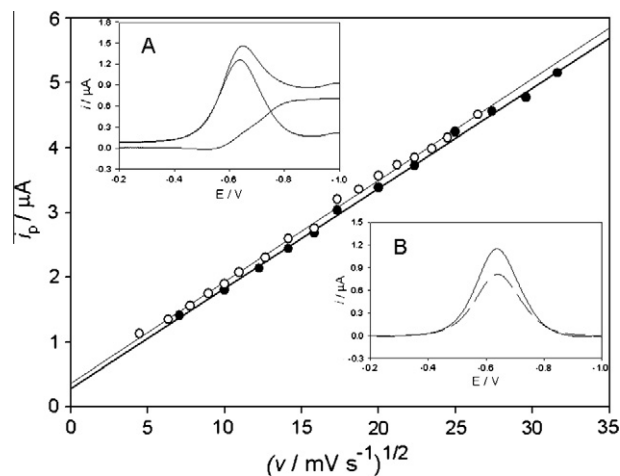


Fig. 8. Dependence of the SW peak height on the formal scan rate for step potentials of 2 (empty points) and 5 mV (full points) at gradually increasing frequency. Solution composition: 0.5 mmol/l Eu^{3+} , 1.0 mol/l NaClO_4 , 0.01 mol/l HClO_4 . Inset (A): a real SW voltammogram (recorded at $f = 10 \text{ s}^{-1}$, $\Delta E = 2$ mV and $E_{sw} = 40$ mV) together with its components. Inset (B): the same voltammogram (solid line) together with the simulated response (dashed line), based on the experimental conditions and parameters determined at the frequency of 100 s^{-1} ($\alpha = 0.5$, $D = 9 \times 10^{-6} \text{ cm}^2 \text{ s}^{-1}$).

unclear. Two lines that reflect measurements performed at two different step potentials and gradually increasing SW frequency show that, for the same scan rate, the peak current obtained with $\Delta E = 2$ mV is always higher than the peak current obtained with $\Delta E = 5$ mV, as follows from the upper expression. The difference between the two values is, however, poorly pronounced (Fig. 8).

The experimental results (from Fig. 8) which do not confirm theoretical predictions could reflect the higher electrode reaction rate than assumed or perhaps the importance of spherical diffusion. Components of the net current, recorded at the lowest SW frequency (10 s^{-1}), are not in agreement with the first assumption (Fig. 8, inset A) indicating that the second possibility is more real. Superimposed theoretical and experimental voltammograms are in good agreement for $f = 100 \text{ s}^{-1}$ (not presented here). At $f = 10 \text{ s}^{-1}$, however, the real signal is significantly higher than the calculated current potential curve (Fig. 8, inset B) when the latter is based on

the experimental conditions (E_{sw} , ΔE , f) and parameters (D , α) used for simulation at the higher frequency. Moreover, the difference between the peak currents of the experimental and calculated voltammograms at $f = 10 \text{ s}^{-1}$ is in a very good agreement with the value of intercept on the y-axis in Fig. 8. (0.34 vs. 0.37 μA for $\Delta E = 2 \text{ mV}$).

5. Conclusions

In staircase voltammetry the gradient of reactant concentration at the working electrode surface decreases with time during each potential step, and its value at the end of the step continuously decreases from step to step until the end of the potential scan. So, the thickness of the diffusion layer at the end of the scan is smaller if the potential step increment is higher and the step duration is shorter. This is the reason why the peak current depends on the square-root of the formal scan rate. However, the proportionality factor is a power function of the potential step increment, as can be seen in Eq. (13), and this is the main difference between staircase voltammetry and linear scan voltammetry.

The formal scan rate $\nu = f \cdot \Delta E$ is not significant parameter in square-wave voltammetry of reversible electrode reactions because mathematical expression of the net peak current consists of two components, the first one being independent of the potential step increment. This is shown in Eq. (22). The first component depends on the concentration gradients of the reactant and product during the cathodic and anodic pulses, respectively. It is a function of the square-root of pulse duration only. Although the reactant consumed in the cathodic pulse is recreated in the anodic pulse, this process is not complete and there is a certain loss of reactant after each pair of pulses. So, the diffusion layer develops during the square-wave scan and its thickness is smaller if the formal scan rate is higher. This is the origin of the second component of the net peak current. The second component is dominant in square-wave voltammetry of totally irreversible electrode reactions because the reactants of these reactions are continuously consumed at both cathodic and anodic pulses. So, the first component vanishes (see Eq. (24)).

Our calculations show that in staircase voltammetry the influences of potential step increment and the step duration on the peak current are not strictly reciprocal, which means that the formal scan rate is not a single variable that determines the response. Furthermore, in square-wave voltammetry of reversible electrode reaction the net peak current depends primarily on the frequency, while the influence of the formal scan rate is of minor importance.

There is, however, an essential difference between reversible and totally irreversible electrode reactions regarding the influence of the potential step increment, or the formal scan rate on the net peak current in square-wave voltammetry.

Taking back to real experiments (which inspired us to perform this study) it seems that much more measurements should be performed in order to find the conditions under which some discrepancy between the theory and practice appears and to find its origin.

Acknowledgement

Financial support of the Ministry of Science, Education and Sports of Republic of Croatia, within the project Electroanalytical investigations of microcrystals and traces of dissolved compounds, is gratefully acknowledged.

References

- [1] A.J. Bard, L.R. Faulkner, *Electrochemical Methods*, second ed., Wiley, New York, 2001.
- [2] H.E. Keller, R.A. Osteryoung, *Anal. Chem.* 43 (1971) 342–348.
- [3] L. Ramaley, M.S. Krause Jr., *Anal. Chem.* 41 (1969) 1362–1365.
- [4] M. Seralathan, R.A. Osteryoung, J.G. Osteryoung, *J. Electroanal. Chem.* 222 (1987) 69–100.
- [5] J.J. Zipper, S.P. Perone, *Anal. Chem.* 45 (1973) 452–458.
- [6] R.S. Nicholson, *Anal. Chem.* 37 (1965) 1351–1355.
- [7] A.W. Bott, *Curr. Separat.* 16 (1997) 23–26.
- [8] E.J. Zachowski, M. Wojciechowski, J. Osteryoung, *Anal. Chim. Acta* 183 (1986) 47–57.
- [9] M.J. Nuwer, J.J. O'Dea, J. Osteryoung, *Anal. Chim. Acta* 251 (1991) 13–25.
- [10] P. Abiman, G.G. Wildgoose, A. Crossley, R.G. Compton, *Electroanalysis* 21 (2009) 897–903.
- [11] A.A. Ensafi, R. Hajian, *Anal. Chim. Acta* 580 (2006) 236–243.
- [12] M. Shahlai, M.B. Gholivand, A. Pourhossein, *Electroanalysis* 21 (2009) 2499–2502.
- [13] J.E. Christie, P.J. Lingane, *J. Electroanal. Chem.* 10 (1965) 176–182.
- [14] M. Seralathan, R. Osteryoung, J. Osteryoung, *J. Electroanal. Chem.* 214 (1986) 141–156.
- [15] R. Bilewicz, K. Wiekil, R. Osteryoung, J. Osteryoung, *Anal. Chem.* 61 (1989) 965–972.
- [16] Z. Stojek, J. Osteryoung, *Anal. Chem.* 63 (1991) 839–841.
- [17] R. Bilewicz, R.A. Osteryoung, J. Osteryoung, *Anal. Chem.* 58 (1986) 2761–2765.
- [18] J.J. O'Dea, J. Osteryoung, R.A. Osteryoung, *Anal. Chem.* 53 (1981) 695–701.
- [19] J. Osteryoung, J.J. O'Dea, in: A.J. Bard (Ed.), *Electroanalytical Chemistry*, vol. 14, Marcel Dekker, New York, 1986, pp. 209–303.
- [20] B. Speiser, in: A.J. Bard, I. Rubinstein (Eds.), *Electroanalytical Chemistry*, Dekker, New York, 1996, pp. 1–108.
- [21] M. Penczek, Z. Stojek, J. Buffle, *J. Electroanal. Chem.* 270 (1989) 1–6.
- [22] N. Fatouros, D. Krulic, H. Groult, *J. Electroanal. Chem.* 625 (2009) 1–6.
- [23] M. Lovrić, *Ann. Chim.* 84 (1994) 379–381.
- [24] M. Zelić, *Croat. Chem. Acta* 76 (2003). and references therein.
- [25] M. Zelić, *Croat. Chem. Acta* 79 (2006) 49–55.
- [26] N. Fatouros, D. Krulic, *J. Electroanal. Chem.* 443 (1998) 262–265.